Available online at www.sciencedirect.com
SCIENCE DIRECT®
ELSEVIER
International Journal of Solids and Structures 41 (2004) 7423–7444
INTERNATIONAL JOURNAL OF SOLIDS and STRUCTURES
www.elsevier.com/locate/ijsolstr

Mechanics and fracture of crack tip deformable bi-material interface

Pizhong Qiao *, Jialai Wang

Department of Civil Engineering, The University of Akron, 244 Sumner Street, Akron, OH 44325-3905, USA

Received 4 December 2003; received in revised form 2 June 2004
Available online 20 July 2004

Abstract

Novel interface deformable bi-layer beam theory is developed to account for local effects at crack tip of bi-material interface by modeling a bi-layer composite beam as two separate shear deformable sub-layers with consideration of crack tip deformation. Unlike the sub-layer model in the literature in which the crack tip deformations under the interface peel and shear stresses are ignored and thus a "rigid" joint is used, the present study introduces two interface compliances to account for the effect of interface stresses on the crack tip deformation which is referred to as the elastic foundation effect; thus a flexible condition along the interface is considered. Closed-form solutions of resultant forces, deformations, and interface stresses are obtained for each sub-layer in the bi-layer beam, of which the local effects at the crack tip are demonstrated. In this study, an elastic deformable crack tip model is presented for the first time which can improve the split beam solution. The present model is in excellent agreements with analytical 2-D continuum solutions and finite element analyses. The resulting crack tip rotation is then used to calculate the energy release rate (ERR) and stress intensity factor (SIF) of interface fracture in bi-layer materials. Explicit closed-form solutions for ERR and SIF are obtained for which both the transverse shear and crack tip deformation effects are accounted. Compared to the full continuum elasticity analysis, such as finite element analysis, the present solutions are much explicit, more applicable, while comparable in accuracy. Further, the concept of deformable crack tip model can be applied to other bi-layer beam analyses (e.g., delamination buckling and vibration, etc.).

Keywords: Bi-material layers; Crack tip element; Crack tip deformation; Interface fracture; Interface joint; Interface deformable bi-layer beam theory

1. Background

A bi-material or bi-layer system is a common configuration in structural applications, and it is usually manufactured by either monolithically forming the two parts together or adhesively bonding the two substrate layers. Interface fracture or interlaminar delamination is one of most common failure modes in

* Corresponding author. Tel.: +1-330-972-5226; fax: +1-330-972-6020.
E-mail address: qiao@uakron.edu (P. Qiao).

0020-7683/$ - see front matter © 2004 Elsevier Ltd. All rights reserved.
doi:10.1016/j.ijsolstr.2004.06.006

this type of layered structures. An elastic joint (crack tip) is formed at the delamination tip of a bi-layer structure where the delaminated portions are connected together with the uncracked portion. Requirement of effective analysis of the local deformation at the crack tip is encountered frequently, such as the delamination buckling of laminated composites (Chai et al., 1981), data reduction technique of fracture tests (Wang and Qiao, 2004a), crack identification (Farris and Doyle, 1993), and vibration analysis of delaminated structures (Brandinelli and Massabo, 2003). A "rigid" joint model is used widely in the literature (Williams, 1988; Suo and Hutchinson, 1990; Schapery and Davidson, 1990), which assumes that the cross-sections at the crack tip remain in one plane and perpendicular to the mid-plane of the virgin beam. This conventional model neglects the elastic deformation of the joint, such as the differential axial extension of the two beams and the root rotation at the crack tip (Sun and Pandey, 1994) and thus forms a rigid joint. Extra errors are introduced, and unfavorable results are obtained by such a conventional split beam model, such as the un-conservative loading of delamination buckling of composites (Shu and Mai, 1993), underevaluated energy release rate of fracture (Sun and Pandey, 1994), and rough dynamic analysis at the crack tip (Farris and Doyle, 1993). The reason of this unfavorable feature of the available elastic "rigid" joint model is explained by the nature of the assumptions used in the beam model, which are unable to describe the severe local deformation at the crack tip of the split beam. As a matter of fact, the local deformation, which is known as the edge effect, is accounted conventionally by Saint-Venant's principle. In the cases where the local deformation is of no interest or of little importance, the conventional rigid joint model is applicable; however, in the cases where the local deformation is significant, a new and improved model is required to account for the elastic deformation at the joint (crack tip). Therefore, Farris and Doyle (1993) pointed out that "a simple scheme to estimate the effective elastic properties of the joint is required", and "this is an area that warrants further study".

Intensive studies have been carried out to accurately model the elastic deformation of a joint (crack tip). For certain simple split beam problem where the beam is symmetric such as a Double Cantilever Beam (DCB) specimen commonly used in mode-I fracture testing, a beam on elastic foundation model proposed by Kanninen (1973, 1974) is usually used in the literature to account for the local deformation at the crack tip (Williams, 1989; Wang and Williams, 1992; Corleto and Hogan, 1995; Ozil and Carlsson, 1999; Qiao et al., 2003a,b). Excellent agreements with numerical finite element analysis and experimental testing results could be reached by this method. However, for a general bi-layer cracked beam, a sub-layer (or sub-laminate in composite laminates) model (Armanios et al., 1986; Wang and Qiao, 2004b,c) is more suitable. In this type of model, each layer of the virgin beam at the joint is modeled as a single sub-beam, instead of only modeling the whole uncracked portion as a composite beam in the conventional way (Suo and Hutchinson, 1990; Schapery and Davidson, 1990). Thus, each layer has individual rotation and the cross-section at the joint does not remain a plane as assumed in the conventional composite beam model (Suo and Hutchinson, 1990; Schapery and Davidson, 1990). In this regard, the joint (crack tip) is deformable and can be analyzed by beam analysis (Wang and Qiao, 2004b). However, the assumption that the interface stresses have no effect on the beam deformation is used in this model (Wang and Qiao, 2004b) leading to a "semi-rigid" joint scenario at the crack tip between two sub-layers. Such a semi-rigid joint model requires two concentrated forces which are nonexistent physically at the crack tip to satisfy the equilibrium condition. Consequently, the local stress distribution is deviating from the actual condition, and the resulting solution of deformation is approximate in nature based on the "semi-rigid" joint model (Wang and Qiao, 2004b). Better accuracy can be achieved by modeling each sub-beam (or sub-laminate) with a higher order beam theory or with more sub-layers. The later approach is referred as multi-sub-layer model since more than two sub-layers are considered, such as proposed by Chatterjee et al. (1986) and Chatterjee and Ramnath (1988) in their study on the mixed mode delamination in composite materials. Improved results could be obtained by this method on interlaminar stress and energy release rate of delamination in composites

if more sub-layers were used in the model. This method was later followed by Zou et al. (2001) through employing the finite element technique, instead of obtaining the governing equation of each sub-layer, and similar improvement in accuracy was demonstrated in their calculations. A very similar approach to the sub-layer model used frequently in the literature is the adhesive joint model (Bruno and Greco, 2001). The only difference between the adhesive joint model and the bi-layer beam model is that the former model employs a linear elastic interface to connect two sub-layers. If the stiffness of interface layer is infinitely large corresponding to a rigid or perfect bonding along the interface, the adhesive joint model coincides with the bi-layer or two-sub-layer model discussed above, and therefore, has the same accuracy.

Some other methods incorporating the crack tip deformation are also available in the literature, which are not so commonly used. Sun and Pandey (1994) obtained an approximate two-dimensional elastic solution for the root rotation at the joint (crack tip) of an isotropic and materially homogeneous split beam. Sundararaman and Davidson (1998) used a torsional spring to describe the deformation at the joint in order to obtain reasonably accurate results in their analysis of an unsymmetric end-notched flexure specimen, in which the stiffness of the torsional spring was obtained numerically. Shu and Mai (1993) used both the "rigid" and "soft" joint models to evaluate the upper and lower bounds of buckling and vibration of a bi-material split beam.

In all the aforementioned investigations, only the model recently developed by the authors (Wang and Qiao, 2004b) provides a simple closed-form solution for general conditions of a bi-layer beam. However, the accuracy of the solution is still low compared to the multi-sub-layer model which has no simple closed-form solution available. To overcome this dilemma, in this study, a novel interface deformable bi-layer theory is proposed to study the complex deformation in the vicinity of the crack tip. Highly accurate closed-form solution of the local deformation near the crack tip is obtained by this model without employing a higher order beam theory or dividing each layer into more sub-layers.

An important application of the crack tip deformation model in interface fracture analysis is discussed in detail in this study also with aim to account for the transverse shear deformation effects on fracture of layered structures. As illustrated most recently by Li et al. (2004), the role of transverse shear force on the interface fracture expressions is fundamentally affected by the local deformation at the crack tip. Although a full continuum elastic analysis (such as finite element analysis) is required to obtain a rigorous solution for the shear component of the ERR (Li et al., 2004), it is feasible that the closed-form solutions of interface fracture considering both the transverse shear and crack tip deformation effects can be obtained analytically by using a proper beam model (Wang and Qiao, 2004b). Armed with the solution of the local deformation at the crack tip obtained in this study, improved closed-form solutions of energy release rate (ERR) and stress intensity factor (SIF) are derived. Compared with the full continuum elasticity analysis, such as finite element analysis of Li et al. (2004), the present solutions are much explicit, more applicable, and comparable in accuracy.

To make the analysis more portable, a segment near the crack tip (i.e., crack tip element) of a split (cracked) bi-layer beam is chosen in this study. This segment is essentially a crack tip element as described by Schapery and Davidson (1990) with a much longer length compared to its thickness so that the far-field boundary condition effect is negligible. This paper is organized as follows: the analytical framework of a novel bi-layer beam theory considering the interface compliances is first established, and the resultant forces and deformations at the crack tip are obtained. To validate the proposed work, the present interface deformable bi-layer beam solution is compared with other available analytical results and numerical finite element analysis. Then the energy release rate of a crack along the interface is obtained based on the deformation solution at the crack tip. The mode decomposition is carried out next, and the explicit expressions of the ERR and SIF are given. Comparisons of fracture parameters (e.g., the ERR and mode mixity) with available numerical analyses are carried out to show the high accuracy of the present solution to interface fracture.

2. Novel interface deformable bi-layer beam theory

Consider a cracked bi-layer beam under general loading of Fig. 1, where a crack lies along the straight interface of the top beam "1" and bottom beam "2" with thickness of h_1 and h_2, respectively. Two beams are made of homogenous, orthotropic materials, with the orthotropy axes along the coordinate system. The length of the uncracked region L is relatively large compared to the thickness of the whole beam $h_1 + h_2$, resulting in the negligible boundary condition effect of the uncracked region on the crack tip is negligible. The length of the delaminated region is not important since it only changes the resultant forces and bending moment at the crack tip. Therefore, in this study it is chosen as infinitesimal for the convenience of analysis. This configuration essentially represents a crack tip element, a small element of a split beam where the cracked and uncracked portions are joined, on which generic loads are applied, as determined by a global beam or beam analysis. It is assumed that a beam theory can be used to model the behavior of the top and bottom layers. A plane stress (beam model) formulation is used in this study, while the plane strain solution can be directly obtained by substituting the proper stiffness and Poisson's ratio.

Considering a typical infinitesimal isolated body of the bi-layer beam system (Fig. 2), the following equilibrium equations are established:

$$\begin{aligned}
&\frac{\mathrm{d}N_1(x)}{\mathrm{d}x} = b\tau(x), \quad \frac{\mathrm{d}N_2(x)}{\mathrm{d}x} = -b\tau(x)\\
&\frac{\mathrm{d}Q_1(x)}{\mathrm{d}x} = b\sigma(x), \quad \frac{\mathrm{d}Q_2(x)}{\mathrm{d}x} = -b\sigma(x)\\
&\frac{\mathrm{d}M_1(x)}{\mathrm{d}x} = Q_1(x) - \frac{h_1}{2}b\tau(x), \quad \frac{\mathrm{d}M_2(x)}{\mathrm{d}x} = Q_2(x) - \frac{h_2}{2}b\tau(x)
\end{aligned} \tag{1}$$

where $N_1(x)$ and $N_2(x)$, $Q_1(x)$ and $Q_2(x)$, $M_1(x)$ and $M_2(x)$ are the internal axial forces, transverse shear forces, and bending moments in layers 1 and 2, respectively; b is the width of the beam; h_1 and h_2 are the thickness of layers 1 and 2, respectively; $\sigma(x)$ and $\tau(x)$ are the interface normal (peel) and shear stresses, respectively.

By making use of the constitutive equations of the individual layers, we can relate the stress resultants and displacements of layers as:

$$N_i = A_i\frac{\mathrm{d}u_i}{\mathrm{d}x}, \quad M_i = D_i\frac{\mathrm{d}\phi_i}{\mathrm{d}x}, \quad Q_i = B_i\left(\phi_i + \frac{\mathrm{d}w_i}{\mathrm{d}x}\right) \tag{2}$$

where A_i, B_i, and D_i $(i = 1, 2)$ are the axial, shear and bending stiffness coefficients of layer i, respectively, expressed as

$$A_i = E_{11}^{(i)}bh_i, \quad B_i = \frac{5}{6}G_{13}^{(i)}bh_i, \quad D_i = E_{11}^{(i)}\frac{bh_i^3}{12}$$

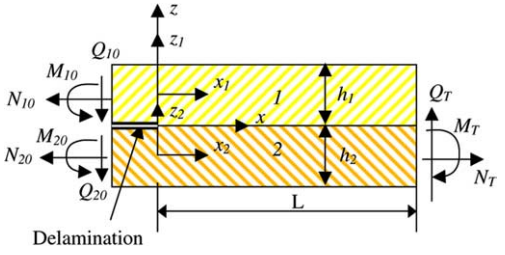

Fig. 1. A crack tip element of bi-material interface under generic loadings.

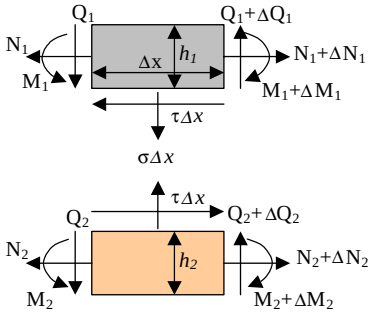

Fig. 2. Free body diagram of a bi-layer beam system.

where $E_{11}^{(i)}$ and $G_{13}^{(i)}$ $(i = 1, 2)$ are the longitudinal Young's modulus and transverse shear modulus of layer i, respectively.

The overall equilibrium requires (Fig. 1)

$$\begin{aligned} &N_1 + N_2 = N_{10} + N_{20} = N_T, \quad Q_1 + Q_2 = Q_{10} + Q_{20} = Q_T \\ &M_1 + M_2 + N_1 \frac{h_1 + h_2}{2} = M_{10} + M_{20} + N_{10} \frac{h_1 + h_2}{2} + Q_T x = M_T \end{aligned} \tag{3}$$

where N_{i0}, Q_{i0} and M_{i0} $(i = 1, 2)$ are the axial forces, transverse shear forces and bending moments in layers 1 and 2 of the cracked portion, respectively; N_T, Q_T and M_T are the resulting forces expressed by the right equality in the above equations.

In the sub-laminate models available in the literature, the first-order shear deformable beam/plate theory is used, in which the effects of interface peel and shear stresses on the crack tip deformation of the beam are ignored (Chatterjee et al., 1986). As a matter of fact, there exists severely concentrated peel and shear stresses along the interface near the crack tip due to the edge effect (Wang and Qiao, 2004b). The large interface stresses at the crack tip can affect the local deformation significantly (Tsai et al., 1998) and make the local deformation at the crack tip very complicated. As a result, the deformation at the crack tip is underestimated by this model. Higher order or multi-layer sub-laminate model can be used to improve the accuracy; however, as a cost, the simplicity in the solutions will be lost.

In this study, with the aim to derive simple closed-form solutions, a novel conception of "interface compliance" first used by Suhir (1986) is employed. As shown in Fig. 3, the real deformed cross-section of each sub-layer is nonlinear, which deviates from the linear one assumed in the first-order shear deformable theory (Wang and Qiao, 2004b). Similarly, Suhir (1986) assumed that the deviation of deformation at any point of the sub-layer interface between the real and the assumed ones using beam theory is proportional to

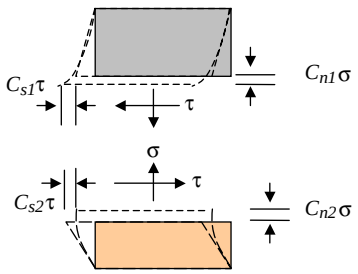

Fig. 3. Displacement continuity conditions along the interface of sub-layers.

the interface stress at that point. Therefore, the displacement continuity along the bi-layer interface has additional contributions from the interface stresses which are taken into account by using two interface compliance coefficients, and is given by (Fig. 3):

$$w_1(x) - C_{n1}\sigma = w_2(x) + C_{n2}\sigma \tag{4}$$

$$u_1(x) - \frac{h_1}{2}\phi_1(x) - C_{s1}\tau = u_2(x) + \frac{h_2}{2}\phi_2(x) + C_{s2}\tau \tag{5}$$

where C_{ni} and C_{si} are the interface compliance coefficients of layer i under the peel and shear stresses, respectively, which account for the contribution of interface stresses to the displacement components at the interface of two layers. The existing sub-laminate model (Armanios et al., 1986; Chatterjee and Ramnath, 1988; Zou et al., 2001; Wang and Qiao, 2004c) is a special case of Eqs. (4) and (5) by assuming the interface compliance coefficients are zero, implying a semi-rigid joint condition, in which only the root rotation is permitted. As a result, the deformation at the crack tip is underestimated (on the rigid side) by the existing sub-laminate model.

It is interesting to point out that the present approach (Eqs. (4) and (5)) in accounting for the effects of interface shear and peel stresses on deformation is similar to a beam on elastic foundation model (Kanninen, 1973, 1974; Williams, 1989), in which the additional deformations due to the interface stresses are captured as "elastic foundation effect" with two foundation stiffnesses. However, the beam on elastic foundation model can only model one sub-beam, while the present study of Eqs. (4) and (5) can model the coupled effects of two sub-layers, and therefore, it is capable of modeling a general mixed mode fracture. In this sense, the present model can be viewed as a generalization of the beam on elastic foundation model. Two interface compliance coefficients can be determined through a semi-analytical and semi-numerical calibrating process as in the elastic foundation model (Corleto and Hogan, 1995). As recently demonstrated by Wang and Qiao (2004a), a good estimation of these two compliances is given by

$$C_{ni} = \frac{h_i}{10E_{33}^{(i)}}, \quad C_{si} = \frac{h_i}{15G_{13}^{(i)}} \tag{6}$$

where $E_{33}^{(i)}$ $(i = 1, 2)$ is the through-the-thickness Young's modulus of layer i. Substituting the first equation in Eqs. (1) and (2) into the second equation of Eq. (5) and differentiating with respective to x yield:

$$\frac{d^2N_1}{dx^2} - bK_s\eta N_1 + bK_s\xi M_1 = -bK_s\left(\frac{N_T}{A_2} + \frac{h_2}{2D_2}M_T\right) \tag{7}$$

where

$$K_s = \frac{1}{C_{s1} + C_{s2}}, \quad K_n = \frac{1}{C_{n1} + C_{n2}}, \quad \xi = \frac{h_1}{2D_1} - \frac{h_2}{2D_2}, \quad \eta = \frac{1}{A_1} + \frac{1}{A_2} + \frac{(h_1 + h_2)h_2}{4D_2}$$

Substituting the third equation in Eqs. (1) and (3) into Eq. (4) and differentiating two more times with respect to x result in:

$$\frac{d^4M_1}{dx^4} + \frac{h_1}{2}\frac{d^4N_1}{dx^4} - bK_n\left(\frac{1}{B_1} + \frac{1}{B_2}\right)\frac{d^2M_1}{dx^2} - \frac{bh_1K_n}{2}\left(\frac{1}{B_1} + \frac{1}{B_2}\right)\frac{d^2N_1}{dx^2} + bK_n\left(\frac{1}{D_1} + \frac{1}{D_2}\right)M_1 + \frac{b(h_1 + h_2)K_n}{D_2}N_1 = \frac{bK_nM_T}{D_2} \tag{8}$$

Combining Eqs. (7) and (8), the governing equation of a bi-layer beam system is established as:

$$\frac{d^6N_1}{dx^6} + a_4\frac{d^4N_1}{dx^4} + a_2\frac{d^2N_1}{dx^2} + a_0N_1 + a_MM_T + a_NN_T = 0 \tag{9}$$

where

$$
\begin{aligned}
a_4 &= -b\left(K_s\left(\frac{\xi h_1}{2}+\eta\right)+K_n\left(\frac{1}{B_1}+\frac{1}{B_2}\right)\right),\\
a_2 &= bK_n\left(K_s\left(\frac{1}{B_1}+\frac{1}{B_2}\right)\left(\eta+\frac{h_1}{2}\xi\right)+\left(\frac{1}{D_1}+\frac{1}{D_2}\right)\right),\\
a_0 &= -b^2K_nK_s\left(\left(\frac{1}{D_1}+\frac{1}{D_2}\right)\eta+\frac{\xi(h_1+h_2)}{2D_2}\right),\\
a_M &= b^2K_nK_s\left(\left(\frac{1}{D_1}+\frac{1}{D_2}\right)\frac{h_2}{2}+\xi\right)\frac{1}{D_2},\\
a_N &= b^2K_nK_s\left(\frac{1}{D_1}+\frac{1}{D_2}\right)\frac{1}{A_2}
\end{aligned}
\tag{10}
$$

Eq. (9) has the same form as the adhesive joint model (Bruno and Greco, 2001). However, in the adhesive joint model, a virtual elastic interface is required with two interface stiffness constants which are served as penalty factors. There is no physical meaning in the interface stiffness constants, and these values are chosen for the convenience of calculation. However, K_s and K_n in this study have a concrete physical implication, and they account for the deformation caused by the interface shear and peel stresses, respectively. Their values can be determined using Eq. (6).

3. Mechanics of crack tip element

3.1. Forces and stresses

The governing differential equation (Eq. (9)) derived in Section 2 can be solved using the characteristic equation:

$$x^6+a_4x^4+a_2x^2+a_0=0 \tag{11}$$

The roots of the above equation for the real material and geometry parameters can be expressed for two cases ((a) and (b)) as: (a) $\pm R_1$, $\pm R_2$ and $\pm R_3$, or (b) $\pm R_1$ and $\pm R_2 \pm \mathrm{i}R_3$. Here R_1, R_2 and R_3 are positive real numbers and $\mathrm{i}=\sqrt{-1}$. In the following, the interface solutions (e.g., N_1) of Eq. (9) based on Cases (a) and (b) are provided.

Case (a): $\pm R_1$, $\pm R_2$ and $\pm R_3$

N_1 in Eq. (9) is expressed as:

$$N_1=\sum_{i=1}^{3}c_i\mathrm{e}^{-R_ix}+\sum_{i=4}^{6}c_i\mathrm{e}^{R_ix}+N_{1C} \tag{12}$$

where c_i $(i=1,2,\ldots,6)$ are the unknown coefficients to be determined by the boundary and continuity conditions. Note that compared to the thickness of the beam, the length of uncracked portion of the bi-layer system is relatively large. Therefore, the terms with positive power in the above equation can be neglected. As a result, we have:

$$N_1=\sum_{i=1}^{3}c_i\mathrm{e}^{-R_ix}+N_{1C},\quad M_1=\sum_{i=1}^{3}c_iS_i\mathrm{e}^{-R_ix}+M_{1C},\quad Q_1=\sum_{i=1}^{3}c_iT_i\mathrm{e}^{-R_ix}+Q_{1C} \tag{13}$$

and

$$S_i = -\frac{R_i^2}{\xi}\frac{1}{bK_s} + \frac{\eta}{\xi}, \quad T_i = R_i\left(\frac{R_i^2}{\xi}\frac{1}{bK_x} - \frac{\eta}{\xi} - \frac{h_1}{2}\right), \quad i = 1,2,3$$

$$N_{1C} = -\frac{a_M}{a_0}M_T - \frac{a_N}{a_0}N_T, \quad M_{1C} = \frac{\eta}{\xi}N_{1C} - \frac{1}{\xi}\left(\frac{N_T}{A_2} + \frac{h_2}{2D_2}M_T\right), \quad Q_{1C} = \frac{\mathrm{d}M_{1C}}{\mathrm{d}x} + \frac{h_1}{2}\frac{\mathrm{d}N_{1C}}{\mathrm{d}x}$$

Considering the overall equilibrium conditions of Eq. (3), we obtain:

$$N_2(x) = -\sum_{i=1}^{3} c_i \mathrm{e}^{-R_i x} + N_{2C}, \quad M_2 = -\sum_{i=1}^{3}\left(S_i + \frac{h_1+h_2}{2}\right)c_i \mathrm{e}^{-R_i x} + M_{2C},$$

$$Q_2(x) = -\sum_{i=1}^{3} c_i T_i \mathrm{e}^{-R_i x} + Q_{2C} \tag{14}$$

where

$$N_{2C} = N_T - N_{1C}, \quad Q_{2C} = Q_T - Q_{1C}, \quad M_{2C} = M_T - M_{1C} - \frac{h_1+h_2}{2}N_{1C}$$

and N_{1C}, M_{1C}, and Q_{1C} are the internal forces of layer 1 based on the conventional composite beam theory (Suo and Hutchinson, 1990). Eq. (13) shows that the resultant forces of sub-layers are composed of two parts: (1) the exponential terms, which decay very fast, representing the local effect; and (2) the stable-state terms (i.e., N_{1C}, M_{1C} or Q_{1C}) from the conventional composite beam solution. At a distance sufficiently far away from the crack tip, the exponential terms are negligible, and the present solution of beam forces in Eq. (13) is therefore reduced to the solution of conventional composite beam theory (Suo and Hutchinson, 1990).

The following conditions at the joint ($x = 0$) are given as:

$$N_1 = N_{10}, \quad M_1 = M_{10}, \quad Q_1 = Q_{10} \tag{15}$$

Then, the coefficients (c_i, i = 1–3) are obtained as:

$$\begin{pmatrix} c_1 \\ c_2 \\ c_3 \end{pmatrix} = \begin{pmatrix} c_{11} & c_{12} & c_{13} \\ c_{21} & c_{22} & c_{23} \\ c_{31} & c_{32} & c_{33} \end{pmatrix}\begin{pmatrix} N \\ M \\ Q \end{pmatrix} = \frac{1}{Y}\begin{pmatrix} S_3T_2 - S_2T_3 & T_3 - T_2 & S_2 - S_3 \\ S_1T_3 - S_3T_1 & T_1 - T_3 & S_3 - S_1 \\ S_2T_1 - S_1T_2 & T_2 - T_1 & S_1 - S_2 \end{pmatrix}\begin{pmatrix} N \\ M \\ Q \end{pmatrix} \tag{16}$$

where $Y = S_2T_1 - S_3T_1 - S_1T_2 + S_3T_2 + S_1T_3 - S_2T_3$ and

$$N = N_{10} - N_{1C}|_{x=0}, \quad M = M_{10} - M_{1C}|_{x=0}, \quad Q = Q_{10} - Q_{1C}|_{x=0} \tag{17}$$

By using equilibrium equation (Eq. (1)), the interface stresses (i.e., peel and shear) are given by:

$$\begin{aligned} \sigma &= \frac{1}{Y}\left(N\sum_{i=1}^{3} R_i T_i c_{i1}\mathrm{e}^{-R_i x} + M\sum_{i=1}^{3} R_i T_i c_{i2}\mathrm{e}^{-R_i x} + Q\sum_{i=1}^{3} R_i T_i c_{i3}\mathrm{e}^{-R_i x}\right) + \sigma_C \\ \tau &= \frac{1}{Y}\left(N\sum_{i=1}^{3} R_i c_{i1}\mathrm{e}^{-R_i x} + M\sum_{i=1}^{3} R_i c_{i2}\mathrm{e}^{-R_i x} + Q\sum_{i=1}^{3} R_i c_{i3}\mathrm{e}^{-R_i x}\right) + \tau_C \end{aligned} \tag{18}$$

Similar to the resulting forces, the interface stresses are expressed in two parts: (1) the exponential terms representing the local stress concentration near the crack tip, and (2) the rest of terms based on the conventional composite beam solution (i.e., σ_C and τ_C).

Case (b): $\pm R_1$ and $\pm R_2 \pm \mathrm{i}R_3$

Similarly, we can obtain the resultant force solutions for this case as:

$$\begin{aligned} N_1 &= c_1 \mathrm{e}^{-R_1 x} + \mathrm{e}^{-R_2 x}(c_2 \cos(R_3 x) + c_3 \sin(R_3 x)) + N_{1C} \\ M_1 &= c_1 S_1 \mathrm{e}^{-R_1 x} + \mathrm{e}^{-R_2 x}(c_2(S_2 \cos(R_3 x) + S_3 \sin(R_3 x)) + c_3(S_3 \cos(R_3 x) + S_2 \sin(R_3 x))) + M_{1C} \\ Q_1 &= c_1 T_1 \mathrm{e}^{-R_1 x} + \mathrm{e}^{-R_2 x}(c_2(T_2 \cos(R_3 x) + T_3 \sin(R_3 x)) + c_3(T_3 \cos(R_3 x) + T_2 \sin(R_3 x))) + Q_{1C} \end{aligned} \tag{19}$$

where

$$S_1 = -\frac{R_1^2}{\xi b K_s} + \frac{\eta}{\xi}, \quad S_2 = -\frac{R_2^2 - R_3^2}{\xi b K_s} + \frac{\eta}{\xi} \quad S_3 = \frac{2R_2 R_3}{\xi b K_s}$$

$$T_1 = -R_1 S_1 - \frac{h_1}{2} R_1, \quad T_2 = -R_2 S_2 + S_3 R_3 - \frac{h_1}{2} R_2, \quad T_3 = -R_2 S_3 + S_2 R_3 - \frac{h_1}{2} R_3 \tag{20}$$

The coefficients of integration c_i are determined by the boundary conditions (Eq. (15)) as:

$$\begin{pmatrix} c_1 \\ c_2 \\ c_3 \end{pmatrix} = \begin{pmatrix} c_{11} & c_{12} & c_{13} \\ c_{21} & c_{22} & c_{23} \\ c_{31} & c_{32} & c_{33} \end{pmatrix} \begin{pmatrix} N \\ M \\ Q \end{pmatrix} = \frac{1}{Y} \begin{pmatrix} S_3 T_2 - S_2 T_3 & T_3 & -S_3 \\ S_1 T_3 - S_3 T_1 & -T_3 & S_3 \\ S_2 T_1 - S_1 T_2 & T_2 - T_1 & S_1 - S_2 \end{pmatrix} \begin{pmatrix} N \\ M \\ Q \end{pmatrix} \tag{21}$$

where $Y = -S_3 T_1 + S_3 T_2 + S_1 T_3 - S_2 T_3$.

3.2. Deformation at crack tip

The deformation at the joint can be obtained from the constitutive law in Eq. (2) and the above solutions of resultant forces of each layer. As an illustration of this process, the rotation of layer 1 at the joint is calculated for Case (a) as:

$$\phi_1(L) - \phi_1(0) = \int_0^L \frac{M_1}{D_1} \mathrm{d}x = \frac{1}{D_1}\left(\frac{c_1 S_1}{R_1} + \frac{c_2 S_2}{R_2} + \frac{c_3 S_3}{R_3}\right) + \int_0^L \frac{M_{1C}}{D_1} \mathrm{d}x \tag{22}$$

Note that:

$$\int_0^L \frac{M_{1C}}{D_1} \mathrm{d}x = \phi_{1C}(L) - \phi_{1C}(0) \tag{23}$$

where ϕ_{1C} is the rotation angle based on the conventional composite beam theory. When L is relatively large, we have:

$$\phi_1(L) = \phi_{1C}(L) \tag{24}$$

Therefore:

$$\phi_{1C}(0) - \phi_1(0) = \Delta\phi_1(0) = S_{21} N + S_{22} M + S_{23} Q \tag{25}$$

where

$$S_{2i} = \frac{1}{D_1}\left(\frac{c_{1i} S_1}{R_1} + \frac{c_{2i} S_2}{R_2} + \frac{c_{3i} S_3}{R_3}\right), \quad i = 1, 2, 3 \tag{26}$$

Following the same procedure as above, we express the deformation of the elastic joint as:

$$\mathbf{\Delta U}(\mathbf{0}) = \mathbf{U}_C(\mathbf{0}) - \mathbf{U}(\mathbf{0}) = \mathbf{SF} \tag{27}$$

where $\mathbf{U}(\mathbf{0}) = \{u_1(0), \phi_1(0), w_1(0), u_2(0), \phi_2(0), w_2(0)\}^{\mathrm{T}}$ represents the displacement components at the crack tip of this study; $\mathbf{U}_C(\mathbf{0}) = \{u_{1C}(0), \phi_{1C}(0), w_{1C}(0), u_{2C}(0), \phi_{2C}(0), w_{2C}(0)\}^{\mathrm{T}}$ represents the displacement components at the crack tip based on the conventional composite beam model;

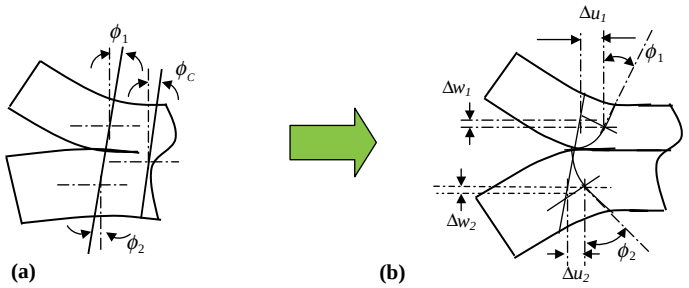

Fig. 4. Joint (crack tip) deformation. (a) Conventional rigid joint; (b) present flexible joint.

$\mathbf{\Delta U}(\mathbf{0}) = \{\Delta u_1(0), \Delta\phi_1(0), \Delta w_1(0), \Delta u_2(0), \Delta\phi_2(0), \Delta w_2(0)\}^{\mathrm{T}}$ are the difference between the conventional composite beam model and the present study; $\mathbf{F} = \{N, M, Q\}^{\mathrm{T}}$ is the loading matrix defined in Eq. (17). $\mathbf{S} = \{S_{ij}\}_{6\times 3}$ is a matrix representing the local deformation compliance at the crack tip and given in Appendix A.

Eq. (27) provides a new continuity condition at the crack tip that is more realistic than that in the conventional composite beam (rigid) model used commonly in the literature (Suo and Hutchinson, 1990) (Fig. 4). As shown in Fig. 4(a), the deformations of each sub-beam at the crack tip are constrained in the conventional rigid joint model such that the deformed cross-section at the crack tip still remains a plane, i.e., the whole joint deforms like a rigid body. On the other hand, the present model (Fig. 4(b)) releases this constraint on the deformations at the crack tip and allows each sub-beam to have different displacement components u_i, w_i and ϕ_i at the crack tip. As a result, the joint behaves like a flexible body, and therefore Eq. (27) is referred to as a flexible joint model in this study.

3.3. Special case: a symmetric bi-layer beam

As an illustration, a simple case of symmetric bi-layer beam is studied in this section. Note that when the two sub-beams have the same material and geometry, i.e., the bi-layer beam is symmetric ($\xi = 0$), and the governing equation (Eq. (7)) is decoupled, thus:

$$\frac{\mathrm{d}^2 N_1}{\mathrm{d}x^2} - bK_{\mathrm{s}}\eta N_1 = -bK_{\mathrm{s}}\left(\frac{N_T}{A_2} + \frac{h_2}{2D_2}M_T\right) \tag{28}$$

The axial force can be obtained as:

$$N_1 = c_1 \mathrm{e}^{-k_1 x} + N_{1C} \tag{29}$$

where

$$k_1 = \sqrt{bK_{\mathrm{s}}\eta} \tag{30}$$

Substituting this solution to Eq. (8), we have:

$$M_1 = c_2 \mathrm{e}^{-k_2 x} + c_3 \mathrm{e}^{-k_3 x} + Sc_1 \mathrm{e}^{-k_1 x} + M_{1C} \tag{31}$$

$$Q_1 = -c_2 k_2 \mathrm{e}^{-k_2 x} - c_3 k_3 \mathrm{e}^{-k_3 x} - \left(S + \frac{h_1}{2}\right) c_1 k_1 \mathrm{e}^{-k_1 x} + Q_{1C} \tag{32}$$

where

$$k_{2,3}=\sqrt{\frac{bK_{\mathrm{n}}\left(\frac{1}{B_1}+\frac{1}{B_2}\right)\pm\sqrt{\left(bK_{\mathrm{n}}\left(\frac{1}{B_1}+\frac{1}{B_2}\right)\right)^2-4bK_{\mathrm{n}}\left(\frac{1}{D_1}+\frac{1}{D_2}\right)}}{2}} \tag{33}$$

$$S=\frac{-\frac{h_1}{2}k_1^4+\frac{bK_{\mathrm{n}}k_1^2h_1^3}{2}\left(\frac{1}{B_1}+\frac{1}{B_2}\right)-\frac{bK_{\mathrm{n}}(h_1+h_2)h_1^4}{2D_2}}{k_1^4-b^2K_{\mathrm{n}}\left(\frac{1}{B_1}+\frac{1}{B_2}\right)k_1^2h_1^2+bK_{\mathrm{n}}\left(\frac{1}{D_1}+\frac{1}{D_2}\right)} \tag{34}$$

The coefficients of integration c_i are determined by the boundary conditions (Eq. (15)) as:

$$\begin{pmatrix}c_1\\c_2\\c_3\end{pmatrix}=\begin{pmatrix}c_{11}&c_{12}&c_{13}\\c_{21}&c_{22}&c_{23}\\c_{31}&c_{32}&c_{33}\end{pmatrix}\begin{pmatrix}N\\M\\Q\end{pmatrix}=\frac{1}{k_2-k_3}\begin{pmatrix}k_2-k_3&0&0\\-(k_1-k_3)S-\frac{h_1}{2}k_1&-k_3&-1\\(k_1-k_2)S+\frac{h_1}{2}k_1&k_2&1\end{pmatrix}\begin{pmatrix}N\\M\\Q\end{pmatrix} \tag{35}$$

The deformation at the crack tip can be expressed by Eq. (27). However, the compliance matrix is different, and it is given by the Case (c) in Appendix A.

3.4. Numerical verification

To verify the above solutions, the deformations at the joint of three simple split beam configurations are examined by the present method and finite element analysis (FEA): (a) a symmetric double cantilever beam (DCB) under unit mode I (open) loading (Fig. 5(a)) with $E_1=E_2=1$, $v_1=v_2=0.3$ and $h_1=h_2=1$; (b) an asymmetric double cantilever beam (ADCB) specimen under mode I loading (Fig. 5(a)) with $E_2=5E_1=5$ and other parameters are the same as Case (a); and (c) an end loaded split (ELS) specimen under mode II loading (Fig. 5(b)) with the same parameters as Case (a). In order to avoid the boundary effect of applied loadings, the geometries in Fig. 5 are chosen as $a/h_1=16$, $a/L=1$. The specimens are modeled by a commercial finite element package ANSYS (1998) as a 2-D problem with 8-node structural plane element (PLANE82). As demonstrated by Table 1 and deformed cross-section (the axial displacement) at the crack tip sketched in Fig. 6, excellent agreements between the present method and FEA have been achieved. Significant rotations at the joint are captured by the present model for the DCB and ADCB specimens; while in the conventional composite beam model, zero joint (crack tip) rotation is assumed. The peel and shear stresses along the interface of two layers are also obtained and presented in Fig. 7. Highly close agreements between the present study and FEA are observed, implying that the present model has an excellent ability to evaluate the interlaminar stresses.

The rotation at the joint plays a significant role in the crack tip element analysis and is of great concern to many researchers (Corleto and Hogan, 1995; Li et al., 2004; Wang and Qiao, 2004b). A highly accurate estimation of rotation at the joint (crack tip) is very desirable, although very few results are available in the literature. Sun and Pandey (1994) obtained a solution of the root rotation at the joint for an isotropic

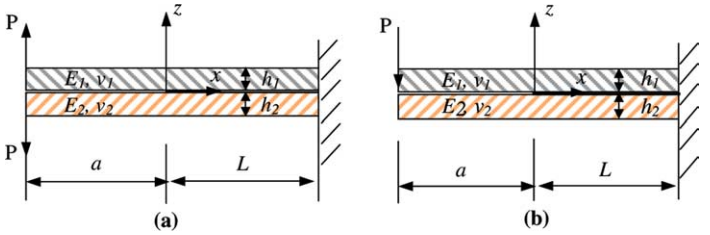

Fig. 5. Specimens under examination. (a) DCB or ADCB specimen; (b) ELS specimen.

Table 1
Displacements and rotations at the joint (present solution and FEA)

Specimen		$E_1h_1\Delta u_1/P$	$E_1h_1\Delta u_2/P$	$E_1h_1\Delta w_1/P$	$E_1h_1\Delta w_2/P$	$E_1h_1^2\Delta\phi_1/P$	$E_1h_1^2\Delta\phi_2/P$
DCB	Present	0.0	0.0	18.3	−18.3	128.8	−128.8
	FEA	0.0	0.0	20.7	−20.7	131.4	−131.4
ADCB	Present	9.74	−1.95	0.54	−20.3	93.0	−42.0
	FEA	7.88	−1.78	1.64	−18.98	97.0	−41.3
ELS	Present	2.5	−2.5	0.0	0.0	14.9	14.9
	FEA	4.16	−4.16	0.0	0.0	13.3	13.3

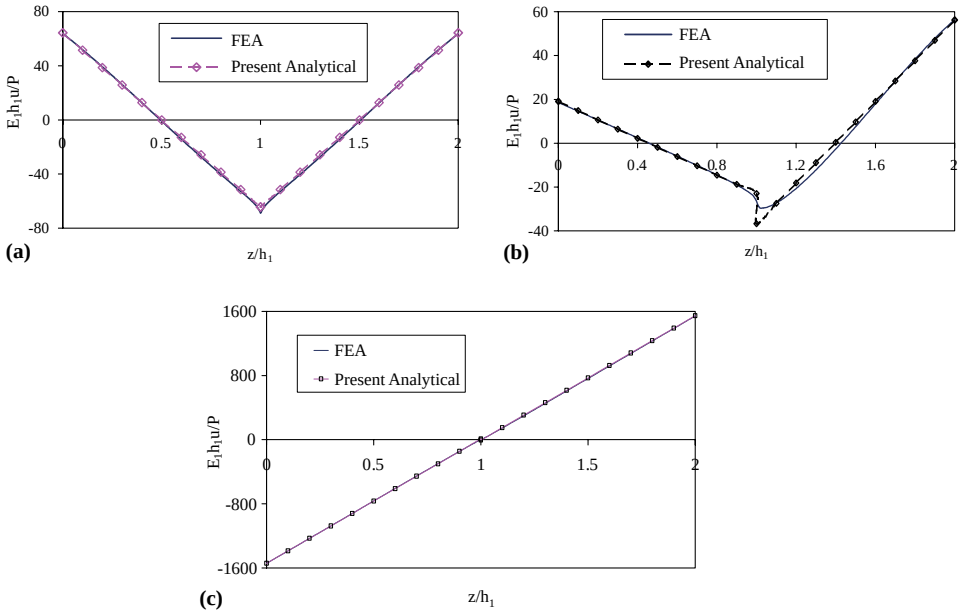

Fig. 6. Comparisons of joint deformation between the present solution and FEA. (a) DCB, (b) ADCB, (c) ELS.

homogeneous split beam under opposite bending moments through an approximate 2-D elastic analysis. The rotation angles obtained by their solution and the present study are shown in Fig. 8 for a range of layer thickness ratios from 0.2 to 5. It can be seen that the present solution is very close to the rotation by the 2-D elastic analysis (Sun and Pandey, 1994). For a general bi-layer situation when the layers are made of different materials and subjected to general loading, there is no analytical solution available in the literature. Recently, Li et al. (2004) obtained a numerical solution of rotation through finite element analysis for isotropic bi-layer joint. In their solution, the rotation at the crack tip is expressed in the same fashion as in Eq. (25). Unlike the present closed-form solution, three nondimensional coefficients in Li et al. (2004) (c_P, c_M and c'_V in their notation as given by the equation in Fig. 9) were obtained by conducting parametric finite element analysis. In Fig. 9, α is Dundurs' (1969) parameter and given by $(E_1/E_2-1)/(E_1/E_2+1)$. Fig. 9 compares the solution by the present study with the coefficients which are determined and noted in the fashion given in Li et al. (2004). An excellent agreement between the present solution and the one by Li et al. (2004) is achieved for the coefficients of the bending moments. Some differences exist for other two coefficients, but the trend is the same. Noting that the bending moment is the most significant loading in rotation, the present solution generally produces very close results to these by FEA.

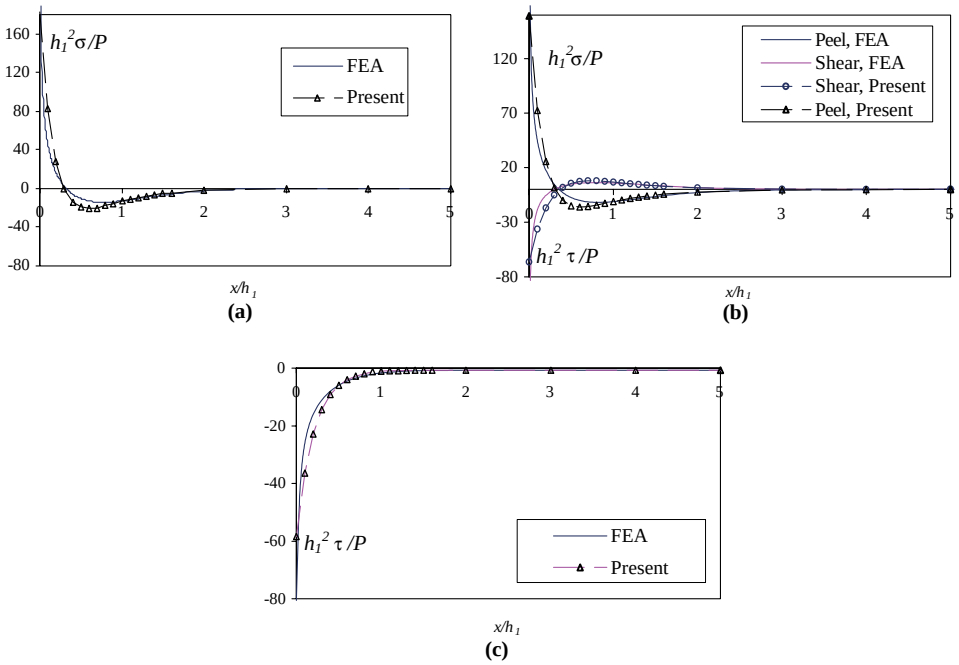

Fig. 7. Interface stresses obtained from the present solution and FEA. (a) DCB, (b) ADCB, (c) ELS.

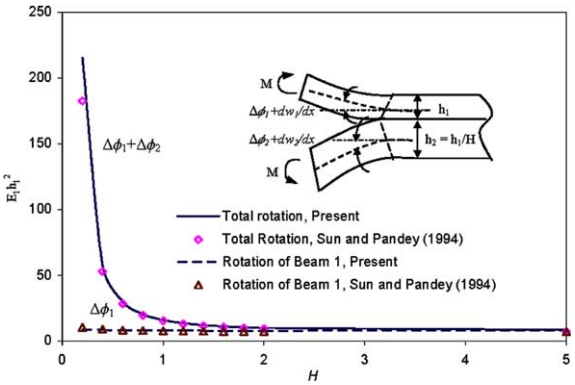

Fig. 8. Comparisons of rotation with different thickness ratios.

4. Interface fracture analysis

Interface cracking is one of common failure modes in multi-layered structures. Typical examples include delamination of composite laminates, debonding of adhesive joints, and decohesion of thin films from substrates. Fracture mechanics principles have been widely employed to assess this type of failure mode in which it is necessary to extract the mode mix of energy release rate (ERR) G and stress intensity factor (SIF) K at the crack tip in order to successfully predict the growth of crack.

Classical beam theory was used in deriving the linear elastic fracture mechanics (LEFM) parameters of interface crack of bi-layer structure in the literature (Suo and Hutchinson, 1990; Schapery and Davidson,

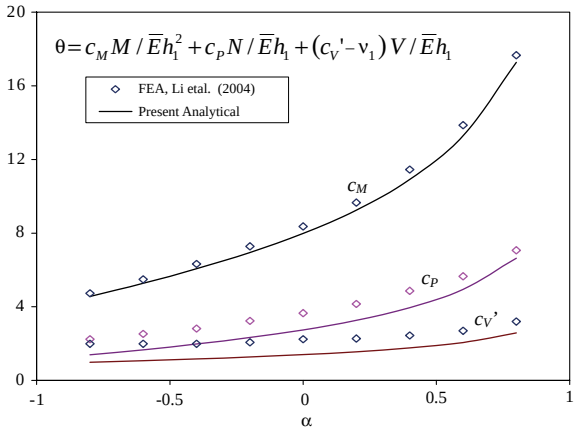

Fig. 9. Coefficients of rotation for beams with different Dundurs' (1969) parameters (α).

1990). However, the effect of transverse shear is not considered in the classical model. A transverse shear force exists at the crack tip in most bi-layer interface fracture problems, such as in a double cantilever beam (DCB) specimen; thus, it has a notable contribution to the ERR and SIF (Gillis and Gilman, 1964; Mostovoy et al., 1967; Kanninen, 1973, 1974). As a matter of fact, the shear deformation effect on the ERR for anisotropic materials with relative low transverse shear modulus such as polymer matrix composite laminates is even more significant as shown in Bruno and Greco (2001) where the portion contributed by the shear deformation was found to be more than half of the total ERR for an orthotropic double cantilever beam specimen. Therefore, it is necessary to account for the contribution from the shear deformation to the ERR, especially when the materials with relative low transverse shear modulus and moderate thickness are concerned. Intensive studies have been carried out to incorporate the transverse shear deformation into the interface fracture expressions (Suo et al., 1991; Bao et al., 1992; Sun and Pandey, 1994; Williams, 1987; Point and Sacco, 1996; Bruno and Greco, 2001; Nilsson et al., 2001). Recently, Wang and Qiao (2004b) presented explicit closed-form solutions of the ERR and SIF which account for the effect of transverse shear force through a novel split beam model based on the first-order shear deformable beam theory. This solution by the shear deformable bi-layer beam theory (Wang and Qiao, 2004b) provides improved and simplified closed-form expressions for the ERR and SIF under the general loading conditions. Compared with a recent numerical analysis carried out by Li et al. (2004), the solution by Wang and Qiao (2004b) still underestimates the ERR, which can be attributed to that the split model used in the formulation is still a semi-rigid joint model. Based on the aforementioned formulation in Section 3, a more flexible split beam or joint model is introduced by the proposed interface deformable bi-layer beam theory, and a more accurate solution of joint deformation obtained is used in this section to derive the ERR, SIF, and mode mixity of interface fracture in a bi-layer beam system.

4.1. Interface fracture parameters

The superposition approach is used in this study to obtain the solution, in which the fracture problem in Fig. 10(a) is divided into two sub-problems of Fig. 10(b)—an uncracked bi-layer beam and Fig. 10(c)—a cracked bi-layer beam only under self-equilibrated forces M, N and Q. Since the uncracked bi-layer beam in Fig. 10(b) produces no ERR, the ERR of Fig. 10(a) equals to that corresponding to Fig. 10(c).

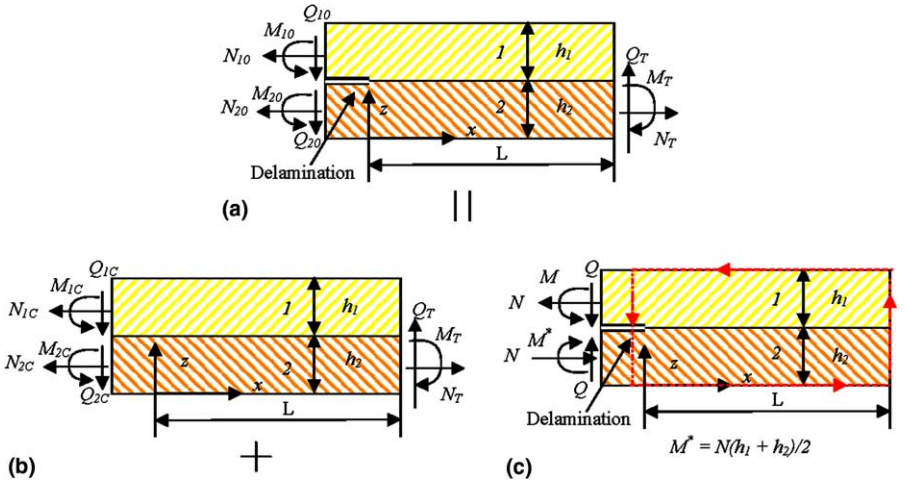

Fig. 10. Equivalent problem of bi-material interface fracture.

The J-integral is used to calculate the energy release rate at the crack tip. A closed path surrounding the crack tip shown in Fig. 10(c) is chosen as the integrating path. The J-integral can be calculated by (Fraisse and Schmit, 1993):

$$J = \frac{1}{2}\left(\frac{N_1^2}{C_1} + \frac{N_2^2}{C_2} + \frac{Q_1^2}{B_1} + \frac{Q_2^2}{B_2} + \frac{M_1^2}{D_1} + \frac{M_2^2}{D_2} - 2Q_1\phi_1 - 2Q_2\phi_2\right)\Big|_{x=L}^{x=0} \tag{36}$$

Substituting the boundary conditions at $x = 0$ and L of the problem in Fig. 10(c), Eq. (36) becomes:

$$J = \frac{1}{2}\left(C_N N^2 + C_M M^2 + C_{MN} MN + \left(\frac{1}{B_1} + \frac{1}{B_2}\right)Q^2 - 2Q(\phi_1(0) - \phi_2(0))\right) \tag{37}$$

where

$$C_N = \frac{1}{C_1} + \frac{1}{C_2} + \frac{(h_1 + h_2)^2}{4D_2}, \quad C_M = \frac{1}{D_1} + \frac{1}{D_2}, \quad C_{MN} = \frac{h_1 + h_2}{D_2} \tag{38}$$

in which the loading parameters M, N, Q are defined by Eq. (17).

It can be seen that the ERR depends not only on the three loading parameters but also the relative rotation at the joint (crack tip). Eq. (37) clarifies the major argument made by Li et al. (2004) on the effects of transverse shear on interface fracture in the layered materials. In their study, Li et al. (2004) pointed out that the crack tip deformation only affects the shear components of the ERR. In this study, two terms of the transverse shear Q are present in Eq. (37) which represent the transverse shear components of the total ERR of the interface fracture: (a) the far-field part $(1/B_1 + 1/B_2)Q^2/2$ which is the contribution of the shear deformation in the cracked region, and (b) $-Q(\phi_1(0) - \phi_2(0))$ which is the contribution from the shear deformation in the uncracked region of a bi-layer beam. Only the latter part (Part (b)) of the transverse shear component is dependent on the local deformation at the crack tip, and more exactly, only dependent on the relative rotation of two sub-layers at the crack tip. It should be noted that the local deformation is not physically a contributor to the ERR. As a matter of fact, the relative rotation in Eq. (37) is a reflection of the complex local stress field, and it disappears once the conventional composite beam model is used. Therefore, the appearance of local deformation in the ERR is the result of the effect of interface stresses

which is ignored in the conventional composite beam model, and thus more transverse shear contribution to the ERR is captured by Eq. (37).

Substituting the solution of rotation at the crack tip (Eq. (25)) obtained in the previous section into Eq. (37), we have:

$$J = \frac{1}{2}\left(C_N N^2 + C_Q Q^2 + C_M M^2 + C_{MN} MN + C_{NQ} NQ + C_{MQ} MQ\right) \tag{39}$$

where

$$C_Q = \frac{1}{B_1} + \frac{1}{B_2} + S_{23} - S_{53}, \quad C_{NQ} = S_{21} - S_{51}, \quad C_{MQ} = S_{22} - S_{52} \tag{40}$$

Compared with the previous study of Wang and Qiao (2004b), the coefficients given in Eq. (40) are larger; thus, the previous study tends to underestimate the ERR.

The energy release rate can be related to the stress intensity factor (Suo, 1990) as:

$$G = \frac{H_{11}}{4\cosh^2(\pi\varepsilon)}|K|^2 \tag{41}$$

Based on the dimensional consideration and linearity, the complex stress intensity factor K can be written in the form:

$$K = K_1 + \mathrm{i}K_2 = \left(\sqrt{C_N}N - \mathrm{i}\mathrm{e}^{\mathrm{i}\gamma_1}\sqrt{C_M}M - \mathrm{i}\mathrm{e}^{\mathrm{i}\gamma_2}\sqrt{C_Q}Q\right)\frac{p}{\sqrt{2}}h_1^{-\mathrm{i}\varepsilon}\mathrm{e}^{\mathrm{i}\omega} \tag{42}$$

where ω is defined in the same way as in Suo and Hutchinson (1990) and

$$\sin(\gamma_1) = \frac{C_{MN}}{2\sqrt{C_M C_N}}, \quad \sin(\gamma_2) = \frac{C_{NQ}}{2\sqrt{C_N C_Q}} \tag{43}$$

It is convenient to use the combination $Kh_1^{\mathrm{i}\varepsilon}$ as suggested by Rice (1988) and define:

$$Kh_1^{\mathrm{i}\varepsilon} = K_{\mathrm{I}} + \mathrm{i}K_{\mathrm{II}} = |K|\mathrm{e}^{\mathrm{i}\psi} \tag{44}$$

Then the stress intensity factors are given by:

$$K_{\mathrm{I}} = \frac{p}{\sqrt{2}}\left(\sqrt{C_N}N\cos(\omega) + \sqrt{C_M}M\sin(\omega+\gamma_1) + \sqrt{C_Q}Q\sin(\omega+\gamma_2)\right) \tag{45}$$

$$K_{\mathrm{II}} = \frac{p}{\sqrt{2}}\left(\sqrt{C_N}N\sin(\omega) - \sqrt{C_M}M\cos(\omega+\gamma_1) - \sqrt{C_Q}Q\cos(\omega+\gamma_2)\right) \tag{46}$$

The phase angle ψ defined is given by:

$$\psi = \tan^{-1}\left(\frac{\sqrt{C_N}N\sin(\omega) - \sqrt{C_M}M\cos(\omega+\gamma_1) - \sqrt{C_Q}Q\cos(\omega+\gamma_2)}{\sqrt{C_N}N\cos(\omega) + \sqrt{C_M}M\sin(\omega+\gamma_1) + \sqrt{C_Q}Q\sin(\omega+\gamma_2)}\right) \tag{47}$$

where

$$\varepsilon = \frac{1}{2\pi}\ln\left(\frac{1-\beta}{1+\beta}\right), \quad \beta = \left([\sqrt{s_{11}s_{33}} + s_{13}]_2 - [\sqrt{s_{11}s_{33}} + s_{13}]_1\right)/\sqrt{H_{11}H_{33}}$$

$$H_{11} = \left[2n\lambda^{\frac{1}{4}}\sqrt{s_{11}s_{33}}\right]_1 + \left[2n\lambda^{\frac{1}{4}}\sqrt{s_{11}s_{33}}\right]_2, \quad H_{33} = \left[2n\lambda^{-\frac{1}{4}}\sqrt{s_{11}s_{33}}\right]_1 + \left[2n\lambda^{-\frac{1}{4}}\sqrt{s_{11}s_{33}}\right]_2 \tag{48}$$

and β is the generalization of one of Dundurs' (1969) parameters for isotropic materials and ε is the bi-material constant. The subscripts "1" and "2" used outside the square brackets in the above expressions

refer to the materials of top and bottom layers, respectively. The nondimensional parameters λ and n are given by:

$$\lambda = \frac{s_{11}}{s_{33}}, \quad n = \sqrt{\frac{1}{2}(1+\rho)}, \quad \rho = \frac{1}{2}\left(\frac{2s_{13}+s_{33}}{\sqrt{s_{11}s_{33}}}\right) \tag{49}$$

where s_{ij} are the material compliance and defined in the conventional fashion.

It can be found that Eqs. (45)–(47) can be reduced to the expressions given in Suo and Hutchinson (1990) if the transverse shear force Q is neglected. In other words, the present results of Eqs. (45)–(47) can be regarded as a straight extension of Suo and Hutchinson's results (1990) which ignore the transverse shear deformation to shear deformable materials. This indicates that the present solution is an improvement of the classical results, and it accounts for the transverse shear deformation in the closed-form solution.

4.2. Comparison and verification

Li et al. (2004) carried out a systematic numerical study of interface fracture in layered materials using finite element analysis. Essentially the same expression as Eq. (39) was obtained in their study but the coefficient C_Q (f_v in their notation) was obtained numerically. The phase angle was calculated through a tedious vector addition process with the aid of an auxiliary angle obtained numerically. Due to the complexity of the interface fracture, especially the effect of β, their solution is only valid to the very simple bi-material interface fracture where the most troublesome, however, inherited feature of interface fracture, oscillation is not present (i.e., $\beta = 0$) and both materials at the bi-layer interface are treated as isotropic. As a comparison, the current analytical solution is applicable in more general situations where the materials

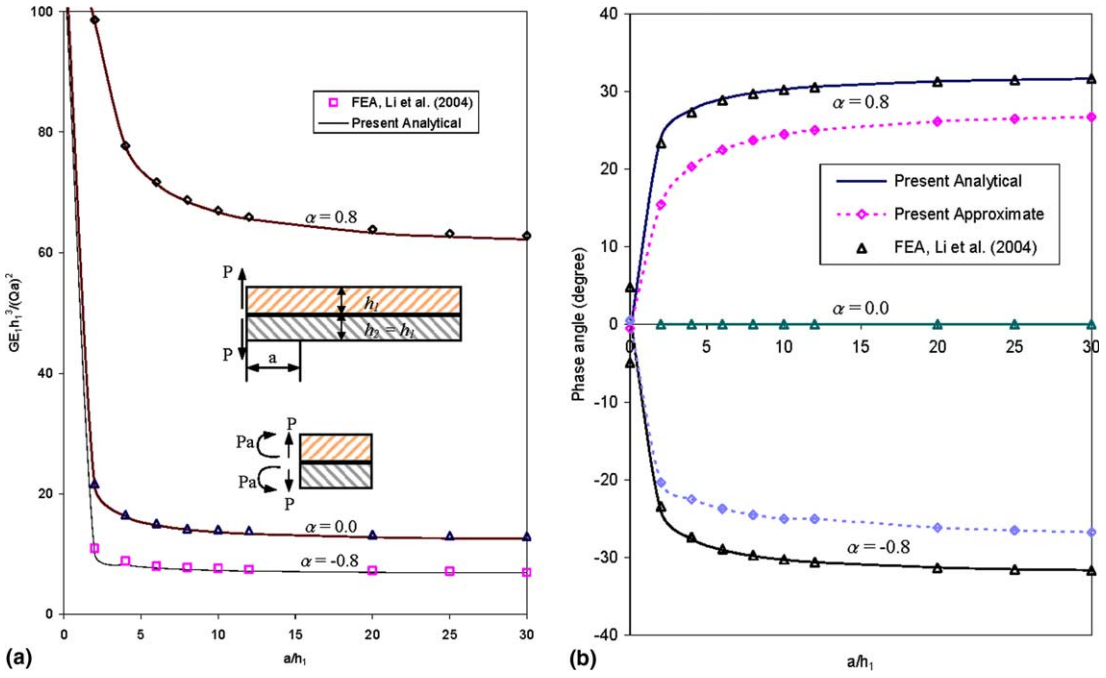

Fig. 11. Comparison of interface fracture parameters for an ADCB specimen. (a) Energy release rate; (b) phase angle.

Table 2
C_Q determined by the present solution and finite element analysis (Li et al., 2004)

α	H									
	0.2		0.4		0.6		0.8		1.0	
	Present	FEA	Present	FEA	Present	FEA	Present	FEA	Present	FEA
−0.8	1.807	1.635	1.800	1.645	1.813	1.663	1.834	1.684	1.861	1.711
−0.6	1.852	1.687	1.840	1.708	1.866	1.739	1.906	1.781	1.952	1.829
−0.4	1.897	1.753	1.894	1.784	1.926	1.836	1.985	1.898	2.049	1.968
−0.2	1.949	1.833	1.939	1.881	1.997	1.954	2.078	2.037	2.163	2.127
0.0	2.009	1.940	2.006	2.009	2.090	2.106	2.191	2.217	2.304	2.335
0.2	2.199	2.089	2.226	2.186	2.350	2.314	2.497	2.460	2.650	2.605
0.4	2.452	2.300	2.531	2.439	2.717	2.619	2.924	2.809	3.133	3.003
0.6	2.839	2.654	3.017	2.865	3.305	3.125	3.608	3.394	3.905	3.665
0.8	3.636	3.412	4.061	3.800	4.583	4.250	5.069	4.704	5.583	5.127

are orthotropic and oscillation is present. The loading parameters for an ADCB specimen shown in Fig. 11(a) are given by Eq. (17) as:

$$N = 0, \quad M = -Pa, \quad Q = -P \tag{50}$$

The interface fracture parameters for this case can then be obtained by Eqs. (39) and (47) as:

$$G = \frac{P^2}{2}\left(C_M a^2 + C_{MQ} a + C_Q\right) \tag{51}$$

$$\psi = -\tan^{-1}\left(\frac{\sqrt{C_M}a\cos(\omega+\gamma_1) + \sqrt{C_Q}\cos(\omega+\gamma_2)}{\sqrt{C_M}a\sin(\omega+\gamma_1) + \sqrt{C_Q}\sin(\omega+\gamma_2)}\right) \tag{52}$$

Table 2 lists the C_Q values obtained by the present analytical solution and finite element results of Li et al. (2004). Generally, these two methods produce very close results and the difference between them is less that 10%. It seems that the present method overestimates C_Q a bit compared with those of Li et al. (2004). This may be attributed to the value of Poisson's ratio chosen in the analytical solution. In this study, a value of Poisson's ratio $v = 0.3$ is fixed for one material and the other ratio is chosen to make $\beta = 0$. The resulting Poisson's ratio is unrealistically large and used to calculate the shear modulus by using $E/2/(1+v)$. Consequently, the transverse shear modulus is relatively small, and the material behaves like orthotropic. As a mater of fact, the current analytical solution can predict almost the same results as the finite element analysis if a realistic Poisson's ratio is chosen in the calculation as shown in Fig. 11. A double cantilever beam (DCB) specimen is studied in Fig. 11 by the present analytical solution which is compared with the finite element results of Li et al. (2004). A value of 0.3 for Poisson's ratio is chosen for both the materials. Both the ERR and phase angle predicted by the present method are in excellent agreements with the FEA results with a maximum error of 1%. Note that the high accuracy of the present solution is valid for the entire material mismatch ranging from $\alpha = -0.8$ to 0.8.

5. Conclusions

In this study, a novel interface deformable bi-layer beam theory is proposed in order to accurately model the crack tip deformation. A bi-layer beam with interface crack is modeled as two separate shear deformable sub-layers bonded perfectly along the interface, and an interface deformable model which

employs two interface compliances at the crack tip is used to account for the effects of the interface stresses on the deformation of the sub-beams (i.e., elastic foundation effect). Closed-form solutions of deformation at the crack tip are obtained. Excellent agreement with full 2-D elastic analysis is reached which validates the accuracy of the present model. Improved solution and analysis of cracked beam are resulted by using the present model. Compared to the rigid joint model based on the conventional composite beam theory (Suo and Hutchinson, 1990; Schapery and Davidson, 1990) and the semi-rigid joint model based on the shear deformable bi-layer beam theory (Wang and Qiao, 2004b), the present flexible join model using the interface deformable bi-layer beam theory shows its accuracy in modeling the actual deformation at the crack tip.

An expression of J-integral of interface fracture in a bi-layer beam is further derived which shows that the shear component of the energy release rate (ERR) depends on the relative rotation of two layers at the crack tip. By substituting the solution of crack tip deformation, closed-form analytical solutions of the ERR and stress intensity factors (SIF) are obtained, for which the transverse shear effect is fully accounted. High accuracy of the present solutions is demonstrated by the remarkable agreements achieved in comparisons with the full elastic study using the finite element analysis for a large range of material mismatch, thickness ratio and material orthotropy. The current solution provides an effective way to retrieve explicit and accurate interface parameters. Further, the interface deformable bi-layer beam theory presented in this study provides analytical solutions for a flexible joint model which can be used effectively in the bi-layer beam analyses (e.g., delamination buckling and vibration, etc.).

Acknowledgements

This study was partially supported by the National Science Foundation (CMS-0002829 and EHR-0090472).

Appendix A. Compliance matrix of elastic joint in Eq. (27)

Case (a): The characteristic Eq. (10) with roots of $\pm R_1$, $\pm R_2$ and $\pm R_3$

$$
\begin{aligned}
S_{1i} &= \frac{1}{A_1}\left(\frac{c_{1i}}{R_1}+\frac{c_{2i}}{R_2}+\frac{c_{3i}}{R_3}\right), \quad i=1,2,3\\
S_{2i} &= \frac{1}{D_1}\left(\frac{c_{1i}S_1}{R_1}+\frac{c_{2i}S_2}{R_2}+\frac{c_{3i}S_3}{R_3}\right), \quad i=1,2,3\\
S_{3i} &= \left(\left(\frac{S_1}{D_1R_1^2}+\frac{T_1}{B_1R_1}\right)c_{1i}+\left(\frac{S_2}{D_1R_2^2}+\frac{T_2}{B_1R_2}\right)c_{2i}+\left(\frac{S_3}{D_1R_3^2}+\frac{T_3}{B_1R_3}\right)c_{3i}\right), \quad i=1,2,3\\
S_{4i} &= -\frac{1}{A_2}\left(\frac{c_{1i}}{R_1}+\frac{c_{2i}}{R_2}+\frac{c_{3i}}{R_3}\right), \quad i=1,2,3\\
S_{5i} &= -\frac{1}{D_2}\left(\frac{c_{1i}S_1}{R_1}+\frac{c_{2i}S_2}{R_2}+\frac{c_{3i}S_3}{R_3}\right)-\frac{h_1+h_2}{2D_2}\left(\frac{c_{1i}}{R_1}+\frac{c_{2i}}{R_2}+\frac{c_{3i}}{R_3}\right), \quad i=1,2,3\\
S_{6i} &= -\left(\left(\frac{\frac{h_1+h_2}{2}+S_1}{D_2R_1^2}+\frac{T_1}{B_2R_1}\right)c_{1i}+\left(\frac{\frac{h_1+h_2}{2}+S_2}{D_2R_2^2}+\frac{T_2}{B_2R_2}\right)c_{2i}+\left(\frac{\frac{h_1+h_2}{2}+S_3}{D_2R_3^2}+\frac{T_3}{B_2R_3}\right)c_{3i}\right), \quad i=1,2,3
\end{aligned}
\tag{A.1}
$$

Case (b): The characteristic Eq. (10) with roots of $\pm R_1$ and $\pm R_2 \pm \mathrm{i}R_3$

$$
\begin{aligned}
S_{1i} &= \frac{1}{A_1}\left(\frac{c_{1i}}{R_1}+\frac{c_{2i}R_2}{R_2^2+R_3^2}+\frac{c_{3i}R_3}{R_2^2+R_3^2}\right), \quad i=1,2,3\\
S_{2i} &= \frac{1}{D_1}\left(\frac{c_{1i}S_1}{R_1}+\frac{c_{2i}(R_2S_2+R_3S_3)}{R_2^3+R_3^2}+\frac{c_{3i}(R_2S_3+R_3S_2)}{R_2^3+R_3^2}\right),\\
&\quad i=1,2,3\\
S_{3i} &= \left(\frac{S_1}{D_1R_1^2}+\frac{T_1}{B_1R_1}\right)c_{1i}+\left(\frac{S_2\left(R_2^2-R_3^2\right)+2R_2R_3S_3}{D_1\left(R_2^2+R_3^2\right)^2}+\frac{T_2R_2+T_3R_3}{B_1(R_2^2+R_3^2)}\right)c_{2i}\\
&\quad +\left(\frac{S_3\left(R_2^2-R_3^2\right)+2R_2R_3S_2}{D_1\left(R_2^2+R_3^2\right)^2}+\frac{T_2R_3+T_3R_2}{B_1(R_2^2+R_3^2)}\right)c_{3i}, \quad i=1,2,3\\
S_{4i} &= -\frac{1}{A_2}\left(\frac{c_{1i}}{R_1}+\frac{c_{2i}R_2}{R_2^2+R_3^2}+\frac{c_{3i}R_3}{R_2^2+R_3^2}\right), \quad i=1,2,3\\
S_{5i} &= -\frac{1}{D_2}\left(\frac{c_{1i}\left(\frac{h_1+h_2}{2}+S_1\right)}{R_1}+\frac{c_{2i}\left(\left(\frac{h_1+h_2}{2}+S_2\right)R_2+R_3S_3\right)}{R_2^3+R_3^2}\right.\\
&\quad \left.+\frac{c_{3i}\left(\left(\frac{h_1+h_2}{2}+S_2\right)R_3+R_2S_3\right)}{R_2^3+R_3^2}\right), \quad i=1,2,3\\
S_{6i} &= -\left(\frac{\frac{h_1+h_2}{2}+S_1}{D_2R_1^2}+\frac{T_1}{B_2R_1}\right)c_{1i}-\left(\frac{\left(\frac{h_1+h_2}{2}+S_2\right)\left(R_2^2-R_3^2\right)+2R_2R_3S_3}{D_2\left(R_2^2+R_3^2\right)^2}-\frac{T_2R_2+T_3R_3}{B_2(R_2^2+R_3^2)}\right)c_{2i}\\
&\quad -\left(\frac{S_3\left(R_2^2-R_3^2\right)+2R_2R_3\left(\frac{h_1+h_2}{2}+S_2\right)}{D_2\left(R_2^2+R_3^2\right)^2}-\frac{T_2R_3+T_3R_2}{B_2(R_2^2+R_3^2)}\right)c_{3i}, \quad i=1,2,3
\end{aligned}
\tag{A.2}
$$

Case (c): Same material and geometry for both sub-layers

$$
\begin{aligned}
S_{1i} &= \frac{1}{A_1}\left(\frac{c_{1i}}{k_1}\right), \quad i=1,2,3\\
S_{2i} &= \frac{1}{D_1}\left(\frac{c_{1i}S}{k_1}+\frac{c_{2i}}{k_2}+\frac{c_{3i}}{k_3}\right), \quad i=1,2,3\\
S_{3i} &= -\frac{1}{B_1}\left(\left(S+\frac{h_1}{2}\right)c_{1i}+c_{2i}+c_{3i}\right)-\frac{1}{D_1}\left(\frac{Sc_{1i}}{k_1^2}+\frac{c_{2i}}{k_2^2}+\frac{c_{3i}}{k_3^2}\right), \quad i=1,2,3\\
S_{4i} &= -\frac{1}{A_1}\left(\frac{c_{1i}}{k_1}\right), \quad i=1,2,3\\
S_{5i} &= -\frac{1}{D_2}\left(\frac{c_{1i}\left(S+\frac{h_1}{2}\right)}{k_1}+\frac{c_{2i}}{k_2}+\frac{c_{3i}}{k_3}\right), \quad i=1,2,3\\
S_{6i} &= \frac{1}{B_2}\left(\left(S+\frac{h_1}{2}\right)c_{1i}+c_{2i}+c_{3i}\right)+\frac{1}{D_2}\left(\frac{\left(S+\frac{h_1}{2}\right)c_{1i}}{k_1^2}+\frac{c_{2i}}{k_2^2}+\frac{c_{3i}}{k_3^2}\right), \quad i=1,2,3
\end{aligned}
\tag{A.3}
$$

References

ANSYS User's Manual Rev. 5.5, vols. I–III, 1998. Swanson Analysis Systems, Inc., Canonsburg, PA.

Armanios, E.A., Rehfield, L.M., Reddy, A.D., 1986. Design analysis and testing for mixed-mode and mode II interlaminar fracture of composites. In: Whitney, J.M. (Ed.), Composite Materials: Testing and Design (Seventh Conference). In: ASTM STP 893. ASTM, Philadelphia, PA, pp. 232–255.

Bao, G., Ho, S., Suo, Z., Fan, B., 1992. The role of material orthotropy in fracture specimens for composites. International Journal of Solids and Structures 29, 1105–1116.

Brandinelli, L., Massabo, R., 2003. Free vibration of delaminated beam-type structures with crack bridging. Composite Structures 61, 129–142.

Bruno, D., Greco, F., 2001. Mixed mode delamination in plates: a refined approach. International Journal of Solids and Structures 38, 9149–9177.

Chai, H., Babcock, C.D., Knauss, W.G., 1981. One dimensional modeling of failure in laminated plates by delamination buckling. International Journal of Solids and Structures 17, 1069–1083.

Chatterjee, S.N., Ramnath, V., 1988. Modeling laminate composite structures as assemblage of sublaminates. International Journal of Solids and Structures 24, 439–458.

Chatterjee, S.N., Pipes, R.B., Dick, W.A., 1986. Mixed mode delamination fracture in laminated composites. Composites Science and Technology 25, 49–67.

Corleto, C.R., Hogan, H.A., 1995. Energy release rates for the ENF specimen using a beam on an elastic foundation. Journal of Composite Materials 29, 1420–1436.

Dundurs, J., 1969. Mathematical theory of dislocations. Journal of Applied Mechanics 36, 650–652.

Farris, T.N., Doyle, J.F., 1993. A global/local approach to length-wise cracked beams: dynamic analysis. International Journal of Fracture 60, 47–156.

Fraisse, R., Schmit, F., 1993. Use of J-integral as fracture parameters in simplified analysis of bonded joints. International Journal of Fracture 63, 59–73.

Gillis, P.P., Gilman, J.J., 1964. Double-cantilever cleavage model of crack propagation. Journal of Applied Physics 35, 647–658.

Kanninen, H.M., 1973. Augmented double cantilever beam model for studying crack propagation and arrest. International Journal of Fracture 9, 83–92.

Kanninen, H.M., 1974. Dynamic analysis of unstable crack propagation and arrest in the DCB specimen. International Journal of Fracture 10, 415–430.

Li, S., Wang, J., Thouless, M.D., 2004. The effects of shear on delamination in layered materials. Journal of the Mechanics and Physics of Solids 52, 193–214.

Mostovoy, S., Crosley, P.B., Rippling, E.J., 1967. Use of crack-line loaded specimens for measuring plane strain fracture toughness. Journal of Materials 2, 661–681.

Nilsson, K.F., Asp, L.E., Alpman, J.E., Nystedt, L., 2001. Delamination buckling and growth for delaminations at different depths in a slender composite panel. International Journal of Solids and Structures 38, 3039–3071.

Ozil, F., Carlsson, L.A., 1999. Beam analysis of angle-ply laminate DCB specimens. Composite Science and Technology 59, 305–315.

Point, N., Sacco, E., 1996. Delamination of beams: an application to the DCB specimen. International Journal of Fracture 79, 225–247.

Qiao, P., Wang, J., Davalos, J.F., 2003a. Analysis of tapered ENF specimen and characterization of bonded interface fracture under Mode-II loading. International Journal of Solids and Structures 40 (8), 1865–1884, Corrigendum: 40(15), 4091.

Qiao, P., Wang, J., Davalos, J.F., 2003b. Tapered beam on elastic foundation model for compliance rate change of TDCB specimen. Engineering Fracture Mechanics 70 (2), 339–353.

Rice, J.R., 1988. Elastic fracture mechanics concepts for interfacial cracks. Journal of Applied Mechanics 55, 98–103.

Schapery, R.A., Davidson, B.D., 1990. Prediction of energy release rate for mixed-mode delamination using classical plate theory. Applied Mechanics Review 43, S281–S287.

Shu, D., Mai, Y., 1993. Buckling of delaminated composites re-examined. Composites Science and Technology 47, 35–41.

Suhir, E., 1986. Stresses in bimetal thermostats. Journal of Applied Mechanics 53, 657–660.

Sun, C.T., Pandey, R.K., 1994. Improved method for calculation strain energy release rate based on beam theorem. AIAA Journal 32, 184–189.

Sundararaman, V., Davidson, B.D., 1998. An unsymmetric end-notched flexure test for interfacial fracture toughness determination. Engineering Fracture Mechanics 60, 361–377.

Suo, Z., 1990. Singularities, interfaces and cracks in dissimilar anisotropic media. Proceedings of the Royal Society of London, Series A—Mathematical Physical and Engineering Sciences A427, 331–358.

Suo, Z., Hutchinson, J.W., 1990. Interface crack between two elastic layers. International Journal of Fracture 43, 1–18.

Suo, Z., Bao, G., Fan, B., Wang, T.C., 1991. Orthotropy rescaling and implications for fracture in composites. International Journal of Solids and Structures 28, 235–248.

Tsai, M.Y., Oplinger, D.W., Morton, J., 1998. Improved theoretical solution for adhesive lap joints. International Journal of Solids and Structures 35, 1163–1185.

Wang, J., Qiao, P., 2004a. Novel beam analysis of end notched flexure specimen for mode-II fracture. Engineering Fracture Mechanics. 71, 219–231.

Wang, J., Qiao, P., 2004b. Interface crack between two shear deformable elastic layers. Journal of the Mechanics and Physics of Solids 52, 891–905.

Wang, J., Qiao, P., 2004c. On the energy release rate and mode mix of delaminated shear deformable composite plates. International Journal of Solids and Structures 41, 2757–2779.

Wang, Y., Williams, J.G., 1992. Correction for mode II fracture toughness specimens of composites materials. Composites Science and Technology 43, 251–256.

Williams, J.G., 1987. Large displacement and end block effects on the 'DCB' interlaminar test in mode I and II. Journal of Composite Materials 21, 330–347.

Williams, J.G., 1988. On the calculation of energy release rate for cracked laminates. International Journal of Fracture 36, 101–119.

Williams, J.G., 1989. End corrections for orthotropic DCB specimens. Composites Science and Technology 35, 367–376.

Zou, Z., Ried, S.R., Soden, P.D., Li, S., 2001. Mode separation of energy rate for delamination in composite laminates using sublaminates. International Journal of Solids and Structures 38, 2597–2613.